

# Lifetime and population of the $2S$ state in muonic hydrogen and deuterium

Marc Diepold,<sup>1</sup> Fernando D. Amaro,<sup>2</sup> Aldo Antognini,<sup>1,3</sup> François Biraben,<sup>4</sup> João M. R. Cardoso,<sup>2</sup> Daniel S. Covita,<sup>5</sup> Andreas Dax,<sup>6</sup> Satish Dhawan,<sup>6</sup> Luis M. P. Fernandes,<sup>2</sup> Adolf Giesen,<sup>7,8</sup> Andrea L. Gouvea,<sup>2</sup> Thomas Graf,<sup>7</sup> Theodor W. Hänsch,<sup>1,\*</sup> Paul Indelicato,<sup>4</sup> Lucile Julien,<sup>4</sup> Cheng-Yang Kao,<sup>9</sup> Paul Knowles,<sup>10</sup> Franz Kottmann,<sup>3</sup> Eric-Olivier Le Bigot,<sup>4</sup> Yi-Wei Liu,<sup>9</sup> José A. M. Lopes,<sup>2,†</sup> Livia Ludhova,<sup>10</sup> Cristina M. B. Monteiro,<sup>2</sup> Françoise Mulhauser,<sup>10,1</sup> Tobias Nebel,<sup>1</sup> François Nez,<sup>4</sup> Paul Rabinowitz,<sup>11</sup> Joaquim M. F. dos Santos,<sup>2</sup> Lukas A. Schaller,<sup>10</sup> Karsten Schuhmann,<sup>3,8,12</sup> Catherine Schwob,<sup>4</sup> David Taqqu,<sup>12</sup> João F. C. A. Veloso,<sup>5</sup> Jan Vogelsang,<sup>1,‡</sup> and Randolph Pohl<sup>1</sup>  
(CREMA collaboration)

<sup>1</sup>*Max-Planck-Institut für Quantenoptik, 85748 Garching, Germany.*

<sup>2</sup>*Departamento de Física, Universidade de Coimbra, 3004-516 Coimbra, Portugal.*

<sup>3</sup>*Institute for Particle Physics, ETH Zurich, 8093 Zurich, Switzerland.*

<sup>4</sup>*Laboratoire Kastler Brossel, École Normale Supérieure, CNRS, and Université P. et M. Curie – Paris 6, Case 74; 4, place Jussieu, 75252 Paris, CEDEX 05, France.*

<sup>5</sup>*IN, Departamento de Física, Universidade de Aveiro, 3810-193 Aveiro, Portugal.*

<sup>6</sup>*Physics Department, Yale University, New Haven, CT 06520-8121, USA.*

<sup>7</sup>*Institut für Strahlwerkzeuge, Universität Stuttgart, 70569 Stuttgart, Germany.*

<sup>8</sup>*Dausinger & Giesen GmbH, Rotebühlstr. 87, 70178 Stuttgart, Germany.*

<sup>9</sup>*Physics Department, National Tsing Hua University, Hsinchu 300, Taiwan.*

<sup>10</sup>*Département de Physique, Université de Fribourg, 1700 Fribourg, Switzerland.*

<sup>11</sup>*Department of Chemistry, Princeton University, Princeton, NJ08544-1009, USA.*

<sup>12</sup>*Paul Scherrer Institute, 5232 Villigen-PSI, Switzerland.*

(Dated: November 5, 2021)

Radiative de-excitation (RD) of the metastable  $2S$  state of muonic hydrogen and deuterium atoms has been observed. In muonic hydrogen, we improve the precision on lifetime and population (formation probability) values for the short-lived  $\mu p(2S)$  component, and give an upper limit for RD of long-lived  $\mu p(2S)$  atoms. In muonic deuterium at 1 hPa,  $3.1 \pm 0.3\%$  of all stopped muons form  $\mu d(2S)$  atoms. The short-lived  $2S$  component has a population of  $1.35^{+0.57}_{-0.33}\%$  and a lifetime of  $\tau_{2S}^{\text{short}}(\mu d) = 138^{+32}_{-34}$  ns. We see evidence for RD of long-lived  $\mu d(2S)$  with a lifetime of  $\tau_{2S}^{\text{long}}(\mu d) = 1.15^{+0.75}_{-0.53}$   $\mu$ s. This is interpreted as formation and decay of excited muonic molecules.

PACS numbers: 36.10.Ee, 31.30.Gs, 33.50.Hv

**Introduction** — When negative muons  $\mu^-$  are stopped in molecular hydrogen ( $\text{H}_2$ ) or deuterium ( $\text{D}_2$ ) gas, muonic hydrogen/deuterium atoms ( $\mu p$ ,  $\mu d$ ) are formed in highly excited states with principal quantum number  $n \approx 14$  [1]. Radiative and collisional de-excitation during the cascade leads to formation of muonic hydrogen atoms in the  $1S$  ground state or the  $2S$  metastable state [2, 3]. The time interval between  $\mu^-$  capture and its arrival in the  $1S$  or  $2S$  state is given by the so-called cascade time  $\tau_{\text{casc}}$ . In muonic hydrogen,  $\tau_{\text{casc}}^{\mu p}$  was measured to be  $37 \pm 5$  ns at 0.6 hPa  $\text{H}_2$  gas pressure [4].

The fraction of muons that actually reach the  $2S$  state can be calculated by the observed x-ray yields during the cascade [5–8]. The fate of these atoms depends on their kinetic energy ( $E_{\text{kin}}$ ): In a collision with a gas molecule,  $2S$  atoms with  $E_{\text{kin}} > 0.3$  eV can end up in the short-lived  $2P$  state which decays immediately to the ground state via Lyman- $\alpha$  ( $K_\alpha$ ) x-ray emission. This 0.3 eV threshold energy in the laboratory frame corresponds to the center-of-mass  $\mu p$   $2S$ - $2P$  Lamb shift splitting of 0.2 eV. These fast de-excited  $2S$  atoms constitute

the so-called short-lived  $2S$  component with a population  $\varepsilon_{2S}^{\text{short}} = 1.70^{+0.80}_{-0.56}\%$  of all created  $\mu p$  atoms, and a lifetime of  $\tau_{2S}^{\text{short}} = 165^{+38}_{-29}$  ns in  $\mu p$  at 0.6 hPa [4].

In contrast,  $2S$  atoms with  $E_{\text{kin}}$  below the threshold constitute the so-called long-lived  $2S$  atoms. In vacuum, the lifetime of the  $\mu p(2S)$  atoms is given by the muon lifetime of  $\tau_\mu \approx 2.2$   $\mu$ s, since the two-photon decay rate is negligibly small. In gaseous environments, collisional processes provide additional decay channels. This was first observed in  $\mu p$ , where a lifetime of  $\tau_{2S}^{\text{long}} \approx 1$   $\mu$ s and a formation probability of  $\varepsilon_{2S}^{\text{long}} = 1.10 \pm 0.08\%$  [9] was measured for this long-lived component at 1 hPa [10]. Such a population was imperative for the measurement of the  $2S$ - $2P$  Lamb shift in muonic hydrogen with laser spectroscopy [11, 12].

The dominant de-excitation mechanism of the long-lived  $\mu p(2S)$  atoms is via non-radiative Coulomb de-excitation (CD) in a collision, leading to  $\mu p(1S)$  atoms with a  $E_{\text{kin}}$  of 900 eV [9, 10, 13]. Such behavior had been predicted as a result of molecular effects [14] via resonant formation of excited muonic molecular ions  $[(pp\mu)^+]$ \* and their subsequent decay. This happens similar to the

Vesman-mechanism [15] which is responsible for muon-catalyzed fusion via the formation of molecular ions from the ground state. Recently, the molecular origin of the observed CD has been questioned, and “direct” CD in a  $\mu p + \text{H}$  collision has been proposed as the source of the observed  $\mu p(1S)$  atoms with  $E_{\text{kin}}$  of 900 eV [16, 17].

Theoretical studies [18, 19] have predicted very different behavior for excited muonic deuterium molecular ions,  $[(dd\mu)^+]*$ , for which no data existed. The dominant de-excitation channel of the excited  $[(dd\mu)^+]*$  ion should be radiative de-excitation (RD) with a branching ratio (BR) around 70%, compared to only about 2% in the excited muonic hydrogen molecular ion  $[(pp\mu)^+]*$ .

Here we report on the measurement of the cascade time, population, and lifetime of both the long-lived and the short-lived  $2S$  state in muonic deuterium,  $\mu d$ , and we provide direct evidence for RD of long-lived  $\mu d(2S)$  atoms. Additionally we give more precise values of the cascade time, population, and lifetime of the short-lived  $2S$  state in  $\mu p$  and provide an upper limit for RD of long-lived  $\mu p(2S)$  atoms.

**Experiment** — The data presented here are acquired during the muonic Lamb shift experiment [11, 12] in 2009. For this experiment low energy muons (3–6 keV kinetic energy) were stopped in a 20 cm long target filled with 1 hPa molecular gas ( $\text{H}_2$  or  $\text{D}_2$ ) at 20°C. Twenty large-area avalanche photo diodes (APDs,  $14 \times 14 \text{ mm}^2$  active area each) [20, 21] placed above and below the target served to detect x-rays between  $\sim 1 \text{ keV}$  and 20 keV that originated from the formed muonic atoms. The 12 APDs with the best x-ray energy resolution of  $\sim 21\%$  (FWHM) at 1.9 keV, and time resolution of 25 ns were used for this analysis, in order to reduce the background as far as possible.

The measured x-ray energies arise from  $K_\alpha$ ,  $K_\beta$ , and  $K_{\geq\gamma}$  lines in  $\mu p$  (1.90, 2.25, and  $\sim 2.45 \text{ keV}$ , respectively) and  $\mu d$  (2.00, 2.36, and  $\sim 2.58 \text{ keV}$ ), silver fluorescence lines near 3 keV, a muonic carbon line ( $\mu\text{C}$ ; 4.75 keV), and various muonic nitrogen ( $\mu\text{N}$ ; 1.01, 1.67, 3.08, 6.65 keV) and muonic oxygen ( $\mu\text{O}$ ; 1.32, 2.19, 4.02, 8.69 keV) transitions. The last two contributions originate from a small leak, creating a 0.55(5)% air admixture in the target gas, that had no influence on the actual Lamb shift measurement. A silver layer on the target cell walls emitted additional delayed x-rays through fluorescence upon contact with muonic atoms.

The primary background source of the experiment derives from muon decay electrons that are detected in the APDs, or in four plastic scintillators, with a time resolution of  $\sim 10 \text{ ns}$ . The offline event selection used in the analysis requires that an eligible x-ray must be followed by the detection of a “delayed” high-energy electron (*del-e*) in a time window  $t_e - t_x \in [0.15 \dots 6] \mu\text{s}$  after the x-ray time (*x-ray + del-e* events). Cuts on the electron identification further minimize the electron-induced background in the x-ray spectra.

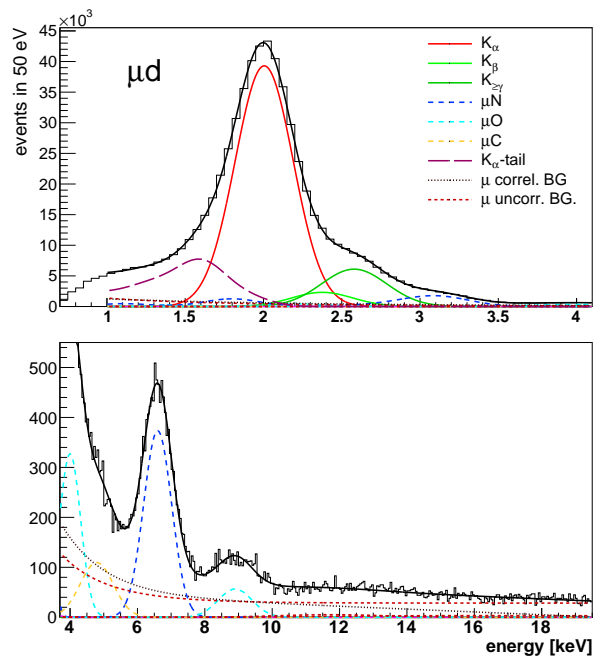


FIG. 1. (Color online) Energy spectrum of all prompt x-rays in the muonic deuterium data. The plot is split to give a better overview over the contributions with low statistics.

**Data analysis and fit results** — Following [4], we first used time-integrated *energy* spectra to determine the shape and position of each of the various  $\mu p/\mu d$ ,  $\text{Ag}$ ,  $\mu\text{C}$ ,  $\mu\text{N}$ , and  $\mu\text{O}$  transitions, as well as shapes of different background contributions. Figure 1 shows the  $\mu d$  data.

In a second step, we used the obtained parameterizations of the energy spectra to fit *time slices* of the *x-ray + del-e* energy spectrum, varying only the amplitudes of x-ray lines and backgrounds. The only exception to this is the position of the  $K_{\geq\gamma}$  line which was found to vary on the order of 50 eV during the time of the prompt peak, as further discussed in the appendix.

The time-dependent x-ray amplitudes and their uncertainties gained by this procedure provide the *time spectra* of the muonic hydrogen  $K_\alpha$  and  $K_{\geq\gamma}$ ,  $\mu\text{O}$ , and  $\mu\text{N}$  x-rays. Sixty time slices of variable length (5 ns to 1  $\mu\text{s}$ , depending on the count rate) span the time up to 9  $\mu\text{s}$  after muon entry. The obtained time spectra are shown in Fig. 2.

To obtain the final results, the  $\mu\text{N}$ ,  $\mu\text{O}$ , and muonic hydrogen  $K_\alpha$  and  $K_{\geq\gamma}$  time spectra were fitted simultaneously (Fig. 2). The  $K_\beta$  spectrum was found to behave as expected but was not further considered here, because it strongly overlaps with both the  $K_\alpha$  and  $K_{\geq\gamma}$  contributions. The fit function used connects different components on the basis of prior knowledge of the muonic atom cascade:

*Muon stop time:* The muon stop time is given by the  $\mu\text{N}$  and  $\mu\text{O}$  time spectra, owing to the negligibly short cascade time  $\sim 10^{-10} \text{ s}$  for these high- $Z$  atoms [22]. The

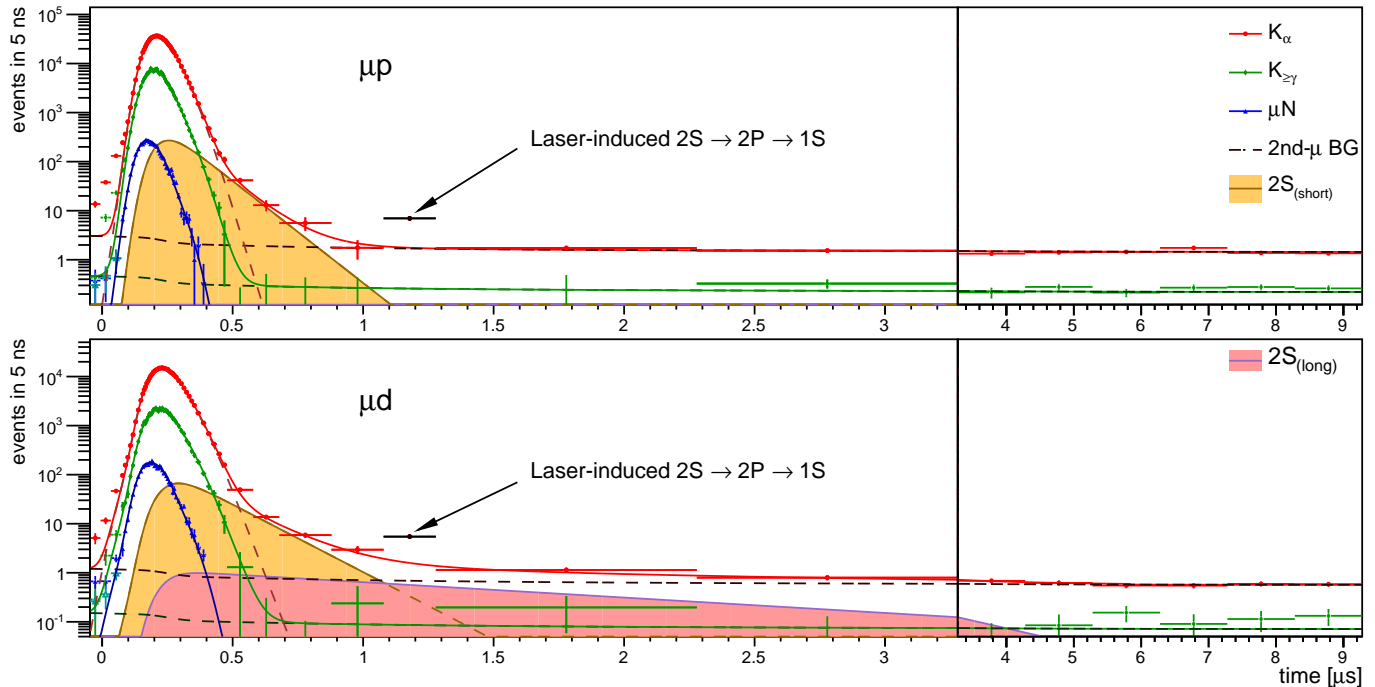


FIG. 2. (Color online) Time spectra and fits for muonic hydrogen (top) and deuterium (bottom). Note the break in the horizontal time axis. The stop time is given by the  $\mu\text{N}$  and  $\mu\text{O}$  (not shown) time spectra. The  $K_{\geq\gamma}$  spectrum is the stop time, convoluted with an (exponential) cascade time distribution. The  $K_{\alpha}$  spectrum in  $\mu p$  shows a short-lived exponential component from radiative quenching of fast  $\mu p(2S)$  atoms. In  $\mu d$ , an additional long-lived component is visible which we consider as evidence for radiative de-excitation of long-lived  $\mu d(2S)$  atoms after formation of excited molecular ions  $[(dd\mu)^+]$ . The  $2S$  components are constructed by the convolution of the  $K_{\geq\gamma}$  distribution with exponential lifetimes (see text). In  $\mu p$  ( $\mu d$ ), the prompt  $K_{\alpha}$  peak contains 881k (412k) events, and the fast component contains 11.6k (4.2k) events. The long-lived component in  $\mu d$  contains 440 events. The fit region starts at  $0.1 \mu\text{s}$  to exclude early-time beam-correlated background.

same phenomenological shape was found to parameterize both the  $\mu\text{N}$  and  $\mu\text{O}$  time spectra with a good  $\chi^2$ .

*Muonic hydrogen/deuterium  $K_{\geq\gamma}$ :* The  $K_{\geq\gamma}$  time spectrum is obtained by convoluting the muon stop time with the  $K_{\geq\gamma}$  cascade time distribution. This distribution is the sum of an exponential with the time constant  $\tau_{\text{casc}}^{\geq\gamma}$ , and a sharp peak at  $t = 0$ , as was suggested by cascade simulations [2, 3]. We find  $\tau_{\text{casc}}^{\geq\gamma} = 27.7 \pm 3.0 \text{ ns}$  and  $28.6 \pm 1.9 \text{ ns}$  for  $\mu p$  and  $\mu d$ , respectively.

Uncorrelated muons stopping in the target at random times give rise to a “2nd- $\mu$ ” background in the  $K_{\geq\gamma}$  time spectrum which is essentially flat at times after the prompt peak. The exact shape has been deduced from the data and shows the expected decrease of event acceptance as a function of time.

*Muonic hydrogen/deuterium  $K_{\alpha}$ :* Prompt peak and 2nd- $\mu$  background of the  $K_{\alpha}$  time spectrum are fitted similarly to the  $K_{\geq\gamma}$  spectrum described above, with the only exception that a purely exponential cascade time distribution is used (no peak at  $t = 0$ ). We find a  $K_{\alpha}$  cascade time  $\tau_{\text{casc}}^{\alpha} = 25.0 \pm 1.5 \text{ ns}$  and  $31.6 \pm 1.7 \text{ ns}$  in  $\mu p$  and  $\mu d$  respectively. These values agree with the respective  $K_{\geq\gamma}$  cascade times, so we forced them to be equal for the final analysis ( $\tau_{\text{casc}}^{\text{avg}}$  in Table I).

In addition,  $K_{\alpha}$  x-rays can originate from fast or slow

RD of the metastable  $2S$  state. The  $2S$  state is populated from the same  $P$  states that produce the  $K_{\geq\gamma}$  x-rays [5], and is modeled to decay (bi-)exponentially. Hence, we use a convolution of the  $K_{\geq\gamma}$  time spectrum with exponentials to parameterize the  $2S$  signal. Short- and long-lived  $2S$  atoms are modeled to give rise to a fast ( $O(100 \text{ ns})$ ) and slow ( $O(1 \mu\text{s})$ ) decay time, respectively.

The time spectrum of *muonic hydrogen* is fitted very well assuming a single fast exponential from the radiatively quenched short-lived  $2S$  states (Fig. 2), with a  $\chi^2/\text{DOF} = 252.5/247$  for the simultaneous fits of all time spectra. The  $K_{\alpha}$  time spectrum alone has a  $\chi^2/\text{DOF}$  of 48.8/48. The fitted amplitude  $\tilde{\epsilon}_{\text{short}}(\mu p) = 1.32_{-0.31}^{+0.42}\%$  and lifetime  $\tilde{\tau}_{\text{short}}(\mu p) = 104_{-13}^{+15} \text{ ns}$  are corrected as described below to obtain the physical values in Table I.

For *muonic deuterium*, both short- and long-lived components have to be included in the  $K_{\alpha}$  fit function to achieve a  $\chi^2/\text{DOF} = 258.5/256$ . The short-lived component has a fitted amplitude  $\tilde{\epsilon}_{\text{short}}(\mu d) = 1.02_{-0.23}^{+0.41}\%$  and lifetime  $\tilde{\tau}_{\text{short}}(\mu d) = 142_{-33}^{+29} \text{ ns}$ . The fitted amplitude of the long-lived component  $\tilde{\epsilon}_{\text{long}}(\mu d) = 0.11_{-0.03}^{+0.07}\%$  is larger than zero with a significance of  $3.8\sigma$ . Its fitted lifetime is  $\tilde{\tau}_{\text{long}}(\mu d) = 1.09_{-0.49}^{+0.70} \mu\text{s}$ . The physical values in Table I include all further corrections.

**Monte Carlo correction** — The apparatus had been optimized for the Lamb shift experiment [11, 12]. For the present analysis of  $2S$  lifetimes and populations, a set of corrections has to be applied to the fit results, in order to gain physical values. As the transverse target dimensions are only  $16 \times 25$  mm<sup>2</sup>, atoms in the  $2S$  state may reach the target cell walls before RD occurs. Both  $1S$  and  $2S$  atoms may also reach the walls after x-ray emission, but before the muon decays. The high- $Z$  target wall materials (Ag and ZnS) favor muon transfer and nuclear muon capture, reducing the  $\mu^-$  decay probability and thus the *x-ray + del-e* rate. This leads to changes of the amplitudes and lifetimes of the observed x-ray signals.

A Monte Carlo simulation (MC) of the experiment was used to determine these loss correction factors of the observed signals. The simulation included the experimental  $E_{\text{kin}}$  distributions of  $\mu p(1S)$  atoms [9, 23], calculated cross sections for both  $\mu p(1S)$  and  $\mu p(2S)$  scattering and  $\mu p(2S)$  quenching [17, 24], as well as the evolution of the atoms'  $E_{\text{kin}}$ , the position-dependent x-ray detection efficiency, and the effect of the delayed electron time window ( $t_e - t_X$ ).

For muonic deuterium we adapted  $\mu p$  parameters with conservative systematic uncertainties. We scaled the initial  $E_{\text{kin}}$  by the reduced mass ratio, a procedure justified due to the similarity of the cascade in  $\mu p$  and  $\mu d$  [25, 26]. Since elastic scattering is unimportant at the low gas pressure of 1 hPa, we also used the  $\mu p$  cross sections in the  $\mu d$  case. According to the MC, detected  $\mu p(2S)$  atoms experience on average only 0.7 elastic collisions before RD occurs. The  $\mu p(1S)$  atoms undergo only 0.3 elastic collisions before muon decay or arrival at the target walls.

The MC revealed that the fitted amplitudes  $\tilde{\varepsilon}_{\text{short}}$  have to be multiplied by  $1.56^{+0.10}_{-0.05}$  ( $\mu p$ ) and  $1.59^{+0.20}_{-0.13}$  ( $\mu d$ ). The fitted lifetimes of the fast components  $\tilde{\tau}_{\text{short}}$  are corrected by  $0.96^{+0.06}_{-0.03}$  ( $\mu p$ ) and  $0.97^{+0.11}_{-0.06}$  ( $\mu d$ ), because the fastest  $2S$  atoms, which contribute most to the signal at early times, may reach the target wall before the beginning of the delayed electron time window.

**X-ray yields** — The lifetimes in Table I are physical lifetimes, corrected as detailed above, but *not* for muon decay. The physical  $2S$  populations ( $\varepsilon$ ) in Table I have been multiplied by  $(1 - \tilde{\tau}/\tau_\mu)$ , where  $\tilde{\tau}$  is the fitted lifetime, to correct for muon decay ( $\tau_\mu = 2.2$   $\mu\text{s}$ ), and by the  $K_\alpha$  yield  $Y_{K_\alpha}/Y_{\text{tot}}$  to normalize to all muons. In  $\mu p$ ,  $Y_{K_\alpha}/Y_{\text{tot}}(\mu p) = 0.803 \pm 0.012$  at 1 hPa is interpolated from the values measured between 0.33 and 8 hPa [7].

In  $\mu d$ , yield measurements existed only for  $\text{D}_2$  gas pressures  $\geq 17$  hPa [8]. We extract the  $\mu d$  yields at 1 hPa from the fitted amplitudes of the prompt  $K_\alpha$ ,  $K_\beta$ , and  $K_{\geq\gamma}$  peaks determined here. Using the  $\mu p$  data and the  $\mu p$  yields allows one to determine the energy-dependent APD detection efficiency. This, together with the prompt amplitudes fitted in  $\mu d$ , gives the  $\mu d$  yields at 1 hPa of

TABLE I. Results for  $\mu p$  and  $\mu d$  at 1 hPa. We give cascade times  $\tau_{\text{casc}}^{\text{avg}}$ , total  $2S$  populations  $\varepsilon_{2S}^{\text{total}}$  obtained from the x-ray yields, and population  $\varepsilon_{2S}^{\text{short}}$  and lifetime  $\tau_{2S}^{\text{short}}$  of the radiatively quenched short-lived  $2S$  atoms. For the population of the long-lived  $\mu d(2S)$  atoms, see text. The populations, but not the lifetimes, have been corrected for  $\mu$ -decay.

	$\mu p$	$\mu d$
$\tau_{\text{casc}}^{\text{avg}}$ (ns)	$25.3 \pm 1.4$	$31.4 \pm 1.8$
$\varepsilon_{2S}^{\text{total}}$ (%)	$2.76 \pm 0.17$ [7]	$3.1 \pm 0.3$
$\varepsilon_{2S}^{\text{short}}$ (%)	$1.73^{+0.56}_{-0.42}$	$1.35^{+0.57}_{-0.33}$
$\tau_{2S}^{\text{short}}$ (ns)	$100^{+16}_{-13}$	$138^{+32}_{-34}$
$\varepsilon_{2S}^{\text{long}}$ (%)	$1.10 \pm 0.08$ [9]	$0.17^{+0.15}_{-0.09}$ (RD) <sup>a</sup>
$\tau_{2S}^{\text{long}}$ ( $\mu\text{s}$ )	$1.04^{+0.29}_{-0.21}$ [10] (CD)	$1.15^{+0.75}_{-0.53}$ (RD)

<sup>a</sup> to be multiplied by  $(1/0.7 \times 8)$  (see Discussion)

$Y_{K_\alpha}/Y_{\text{tot}} = 0.78 \pm 0.02$ ,  $Y_{K_\beta}/Y_{\text{tot}} = 0.06 \pm 0.01$ , and  $Y_{K_{\geq\gamma}}/Y_{\text{tot}} = 0.16 \pm 0.03$ . As expected, the  $\mu p$  and  $\mu d$  x-ray yields are very similar [8, 25, 26].

**Discussion** — For muonic *hydrogen* we find a cascade time of  $\tau_{\text{casc}}^{\mu p} = 25.3 \pm 1.4$  ns and a radiatively quenched short-lived  $2S$  population of  $\varepsilon_{2S}^{\text{short}}(\mu p) = 1.73^{+0.56}_{-0.42}\%$  with lifetime  $\tau_{2S}^{\text{short}}(\mu p) = 100^{+16}_{-13}$  ns (Table I). These values (if gas pressure difference scaling is included) agree with, yet are more precise than, those in Ref. [4].

The  $\mu p$  data are well fitted assuming no radiative quenching of long-lived  $\mu p(2S)$  atoms. This agrees with previous observations [10] that long-lived  $\mu p(2S)$  atoms quench mainly via CD, an effect explained both by direct CD [17] and molecular CD [14, 18, 19]. Theory predicts that an excited  $[(pp\mu)^+]$  molecule decays mainly via CD, with a radiative BR of only 2% in muonic hydrogen [18, 19], an effect too small to observe in the present experiment, or in previous searches for RD of long-lived  $\mu p(2S)$  atoms [5, 6].

The radiatively quenched short-lived  $\mu p(2S)$  atoms observed here,  $\varepsilon_{2S}^{\text{short}}(\mu p) = 1.73^{+0.56}_{-0.42}\%$ , and the long-lived  $\mu p(2S)$  population from Ref. [9],  $\varepsilon_{2S}^{\text{long}}(\mu p) = 1.10 \pm 0.08\%$ , sum to  $\varepsilon_{2S}^{\text{total}}(\mu p) = 2.8^{+0.6}_{-0.4}\%$ , in agreement with the total  $\mu p(2S)$  population at 1 hPa,  $\varepsilon_{2S}^{\text{total}}(\mu p) = 2.76 \pm 0.17\%$ , calculated from the K-x-ray yields [7].

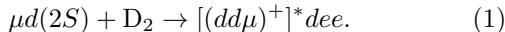
For muonic *deuterium* we determine a cascade time of  $\tau_{\text{casc}}^{\mu d} = 31.4 \pm 1.8$  ns and a radiatively quenched short-lived  $2S$  population of  $\varepsilon_{2S}^{\text{short}}(\mu d) = 1.35^{+0.57}_{-0.33}\%$  with lifetime  $\tau_{2S}^{\text{short}}(\mu d) = 138^{+32}_{-34}$  ns. The short-lived amplitude agrees with the one observed in  $\mu p$ .

Both the cascade time and lifetime of the short-lived  $2S$  atoms scale as  $\sqrt{m(\mu d)/m(\mu p)} = 1.38$ , as expected for velocity-dependent collisional processes of  $\mu p$  and  $\mu d$  atoms with similar  $E_{\text{kin}}$ .

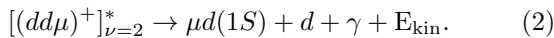
The long-lived component observed in  $\mu d$  is direct evidence for RD of long-lived (slow)  $\mu d(2S)$  atoms. Its lifetime  $\tau_{2S}^{\text{long}}(\mu d) = 1.15^{+0.75}_{-0.53}$   $\mu\text{s}$  is in good agreement

with the CD signal lifetime observed in  $\mu p$ ,  $\tau_{2S}^{\text{long}}(\mu p) = 1.04^{+0.29}_{-0.21}$   $\mu\text{s}$  at 1 hPa [9, 10].

The total  $\mu d(2S)$  population at 1 hPa is  $\varepsilon_{2S}^{\text{total}}(\mu d) = 3.1 \pm 0.3\%$ , calculated from the  $\mu d$  yields measured here. The difference  $\varepsilon_{2S}^{\text{total}} - \varepsilon_{2S}^{\text{short}} = 1.7^{+0.4}_{-0.7}\%$  is the *expected* long-lived  $\mu d(2S)$  population. It agrees with the value measured in  $\mu p$ ,  $\varepsilon_{2S}^{\text{long}}(\mu p) = 1.10 \pm 0.08\%$  [9]. Also, the size of the laser-induced  $2S \rightarrow 2P \rightarrow 1S$  signals (Fig. 2) proves that the long-lived  $2S$  population is very similar in  $\mu p$  and  $\mu d$ . The observed long-lived amplitude,  $\varepsilon_{2S}^{\text{long}} = 0.17^{+0.15}_{-0.09}\%$  is  $\sim 10$  times smaller than the expected amplitude. This can be explained via molecular formation from the excited  $\mu d(2S)$  state in a collision with  $D_2$ ,



Subsequent Auger-emission of both electrons leads to the formation of a  $[(dd\mu)^+]^*$  molecular ion in a  $1S^e$  state of the  $3d\sigma_g$  potential, with vibrational quantum number  $\nu = 2$  [13, 18, 19]. This state decays with a radiative BR of  $\sim 70\%$  into the anti-binding  $2p\sigma_u$  potential [18, 19]



The Franck-Condon principle predicts the x-ray spectrum in Fig. 5 of Ref. [19]. Moreover, the decay into the anti-binding  $2p\sigma_u$  potential produces *accelerated*  $\mu d(1S)$  atoms. These can hit the walls before muon decay occurs which suppresses the observed signal amplitude for the *x-ray + del-e* event class. The MC predicts that acceleration to 15 eV will give the observed factor of 1/7.

From the wave function [19, 27] one finds that 27%, 8%, and 65% of the  $\mu d(1S)$  atoms formed by RD from the  $\nu = 2$  state acquire a  $E_{\text{kin}}$  of 2.1, 16, and 56 eV, giving signal reduction factors of 0.34, 0.10, and 0.03, respectively. This results in an overall signal reduction of 1/8, in agreement with the observed factor of 1/7.

For muonic hydrogen, the absence of a long-lived radiative component in the present data corresponds to a radiative BR that is at least 3.5 times smaller (90% C.L.) in  $[(pp\mu)^+]^*$  than the one observed in  $[(dd\mu)^+]^*$ .

The observed lifetime of the long-lived  $2S$  component,  $\tau_{2S}^{\text{long}} \approx 1$   $\mu\text{s}$  at 1 hPa both in  $\mu p$  [10] and  $\mu d$ , is given by the excited muonic molecules formation rate (Eq. (1)) [28]. Auger emission and RD/CD (Eq. (2)) are much faster [18, 19].

**Conclusion** — Comparison of cascade times, yields, lifetimes, and populations of the short- and long-lived  $2S$  atoms presented here shows that the cascade in muonic hydrogen and deuterium is very similar [25, 26]. A notable exception is the de-excitation of the long-lived  $2S$  state, which proceeds mainly via RD of  $[(dd\mu)^+]^*$  molecules in  $\mu d$ , in contrast to CD in  $\mu p$  [10].

Molecular effects have proven to be important in muonic hydrogen scattering in gas targets [9, 29], as well as during muon-catalyzed fusion [15, 30, 31]. The

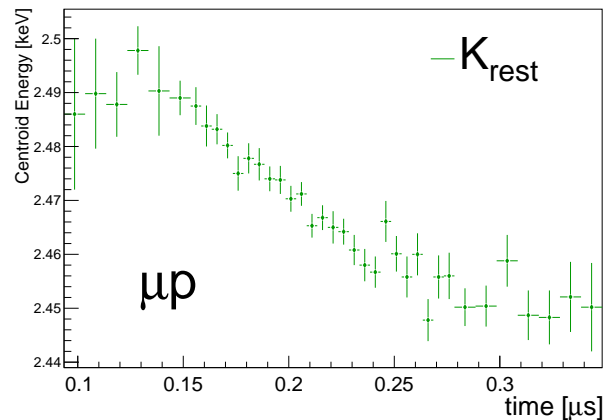


FIG. 3. (Color online) Centroid energy of the  $K_{\geq\gamma}$  component as obtained by the fit of the  $\mu p$  dataset between 0.1 and 0.4  $\mu\text{s}$  after muon entry.

present analysis demonstrates the prominence of molecular effects in excited state processes of muonic hydrogen atoms. The measured formation rate of excited muonic molecules,  $\lambda \approx 0.5 \times 10^6$   $\text{s}^{-1}$ , at 1 hPa gas pressure is large, and at gas pressures approaching liquid hydrogen density, as many as 65% of the muons populate the metastable  $2S$  state [3]. Hence, formation and decay of excited muonic molecules from states with  $n \geq 2$  is expected to have a strong influence on the cascade and dynamics of muonic hydrogen isotopes [3, 14].

#### Appendix: Energy shift of the $K_{\geq\gamma}$ component

— While fitting the *time slices* of the *x-ray + del-e* energy spectra, it became apparent that a fixed parameterization of the  $K_{\geq\gamma}$  contribution was not suitable to describe the data on a satisfactory level. In order to improve the quality of the fit, the centroid energy of the  $K_{\geq\gamma}$ -peak was treated as a free parameter in the high statistics region of the datasets. As can be seen in Fig. 3, the energy of the  $K_{\geq\gamma}$  contribution is  $2.49 \pm 0.01$  keV at times shortly after the muon entry, but then declines to  $2.45 \pm 0.01$  keV for the latest cascade times in the case of  $\mu p$ . This can be explained by recollecting that muonic hydrogen atoms are created in highly excited states [1] and de-excite in the cascade through different processes [2, 3]. At early time directly after muonic atom formation,  $K_{\geq\gamma}$  transitions start mainly from high  $n$ -levels ( $n \sim 7-12$ ) corresponding to transition energies near the  $\mu p(1S)$  dissociation energy of 2.53 keV. Lower initial  $n$ -levels ( $n \sim 4-7$ ) dominate at later times, leading to the corresponding lower transition energies.

**Acknowledgments** — The authors thank V.P. Popov and V.N. Pomerantsev for the  $\mu p(1S)$  and  $\mu p(2S)$  cross sections used in the MC as well as J.P. Karr and L. Hilico for the results of their calculation and fruitful discussions. We acknowledge support from the European Research Council (ERC) under grant StG. 279765, the Swiss National Science Foundation

(projects 200020–100632 and 200021L–138175/1), the Swiss Academy of Engineering Sciences, the BQR de l’UFR de physique fondamentale et appliquée de l’Université Paris 6, the program PAI Germaine de Staël no. 07819NH du ministère des affaires étrangères France, and the FCT and FEDER under grant SFRH/BPD/46611/2008 and project FIS/82006/2006. P.I. acknowledges support by the “ExtreMe Matter Institute, Helmholtz Alliance HA216/EMMI”. T.W.H. acknowledges support from the Max–Planck–Society and the Max–Planck–Foundation. Laboratoire Kastler Brossel is “UMR n° 8552” of the ENS, CNRS and UPMC.

---

\* also at Ludwig-Maximilians-Universität, Munich, Germany.

† also at Instituto Politécnico de Coimbra, ISEC, 3030–199, Portugal.

‡ present address: Institut für Physik, Carl von Ossietzky Universität, 26129 Oldenburg, Germany.

- [1] M. Leon and H. A. Bethe. *Phys. Rev.* **127**, 636 (1962).
- [2] T. S. Jensen and V. E. Markushin. *Eur. Phys. J. D* **21**, 261 (2002).
- [3] T. S. Jensen and V. E. Markushin. *Eur. Phys. J. D* **21**, 271 (2002).
- [4] L. Ludhova, et al. *Phys. Rev. A* **75**, 040501 (2007).
- [5] H. Anderhub, et al. *Phys. Lett. B* **71**, 443 (1977).
- [6] P. O. Egan, et al. *Phys. Rev. A* **23**, 1152 (1981).
- [7] H. Anderhub, et al. *Phys. Lett. B* **143**, 65 (1984).
- [8] M. Bregant, et al. *Phys. Lett. A* **241**, 344 (1998).
- [9] R. Pohl. Ph. D. thesis #14096, ETH Zurich, Switzerland (2001), online at <http://e-collection.ethbib.ethz.ch>.
- [10] R. Pohl, et al. *Phys. Rev. Lett.* **97**, 193402 (2006).
- [11] R. Pohl, et al. *Nature* **466**, 213 (2010).
- [12] A. Antognini, et al. *Science* **339**, 417 (2013).
- [13] R. Pohl, et al. *Hyp. Interact.* **138**, 35 (2001).
- [14] P. Froelich and A. Flores-Riveros. *Phys. Rev. Lett.* **70**, 1595 (1993).
- [15] E. A. Vesman. *Pis'ma Zh. Eksp. Teor. Fiz.* **5**, 113 (1967). [*JETP Lett.* **5**, 91 (1967)].
- [16] G. Ya. Korenman, V. N. Pomerantsev, V. P. Popov. *JETP Lett.* **81**, 543 (2006).
- [17] V. P. Popov and V. N. Pomerantsev. *Phys. Rev. A* **83**, 032516 (2011).
- [18] E. Lindroth, J. Wallenius, and S. Jonsell. *Phys. Rev. A* **68**, 032502 (2003). Erratum *ibid.* **69**, 059903(E) (2004).
- [19] S. Kilic, J.-P. Karr, and L. Hilico. *Phys. Rev. A* **70**, 042506 (2004).
- [20] L. Fernandes, et al. *Nucl. Inst. Meth. A* **498**, 362 (2003).
- [21] L. Ludhova, et al. *Nucl. Inst. Meth. A* **540**, 169 (2005).
- [22] L. Bracci and G. Fiorentini. *Nuovo Cimento A* **43**, 9 (1978).
- [23] F. Kottmann, et al. *Hyp. Interact.* **119**, 3 (1999).
- [24] V. P. Popov and V. N. Pomerantsev. private comm.
- [25] B. Lauss, et al. *Phys. Rev. Lett.* **80**, 3041 (1998).
- [26] B. Lauss, et al. *Phys. Rev. A* **60**, 209 (1999).
- [27] J.-P. Karr and L. Hilico. private comm.
- [28] J. Wallenius, S. Jonsell, Y. Kino and P. Froelich. *Hyp. Interact.* **138**, 285 (2001).
- [29] A. Adamczak, et al. *At. Data and Nucl. Data Tables* **62**, 225 (1996).
- [30] L. I. Ponomarev. *Contemp. Phys.* **32**, 219 (1990).
- [31] D. Balin, et al. *Phys. Part. Nucl.* **42**, 185 (2011).